

## Supporting information

# Biodegradable Hollow MoSe<sub>2</sub>/Fe<sub>3</sub>O<sub>4</sub> Nanospheres as PDT Enhanced Agent for Multimode CT/MR/IR Imaging and Synergistic Anti-Tumor Therapy

Ying Wang<sup>1</sup>, Feng Zhang<sup>1</sup>, Huiming Lin<sup>1,2\*</sup>, and Fengyu Qu<sup>1\*</sup>

*1. Key Laboratory of Photochemical Biomaterials and Energy Storage Materials and College of*

*Chemistry and Chemical Engineering, Harbin Normal University, Harbin 150025, China*

*2. Laboratory for Photon and Electronic Bandgap Materials, Ministry of Education, Harbin*

*Normal University, Harbin 150025, China*

E-mail: [qufengyu@hrbnu.edu.cn](mailto:qufengyu@hrbnu.edu.cn) and [linhuiming@hrbnu.edu.cn](mailto:linhuiming@hrbnu.edu.cn)

## EXPERIMENTAL SECTION

### Chemicals and Materials

Unless specified otherwise, all of the chemicals used were of analytical grade and used without further purification. Sodium molybdate ( $\text{Na}_2\text{MoO}_4$ , anhydrous, 98+%, STREM). Selenium powder (Se, > 99%), iron(III) acetylacetonate ( $\text{Fe}(\text{acac})_3$ , 98%), dichlorofluorescein diacetate (DCFH-DA), methoxypolyethylene glycol amine, PEI ( $M_w = 1800$ , 99%) and diethylene glycol (DEG, 99%) were purchased from Aladdin Co. Ltd. Hydrazine hydrate ( $\text{N}_2\text{H}_4 \cdot \text{H}_2\text{O}$ , 50 wt %, sinopharm Chemical Reagent Co. Ltd). Calcein acetoxymethyl ester (calcein AM, KeyGEN BioTCH). Propidium iodide (PI, Alfa Aesar). Doxorubicin hydrochloride ( $\text{DOX} \cdot \text{HCl}$ ) and 3-(4,5-dimethyl-2-thiazolyl)-2,5-diphenyl-2-Htetrazolium bromide (MTT) were purchased from Sigma Aldrich Co. Ltd.

### Synthesis of hollow $\text{MoSe}_2$ nanospheres

The hollow  $\text{MoSe}_2$  nanospheres were synthesized by a facile solvothermal reaction method. Briefly, 0.126 mmol of selenium powders were added into 5 mL of hydrazine hydrate and stirring for 1 h at 80 °C to form the Se-precursor solution. At the same time, 0.063 mmol of  $\text{Na}_2\text{MoO}_4$  was dispersed in 15 mL of DMF with a violent stirring. Then, 5 mL of Se solutions were dropwise added into the above Mo solution. Finally, the above mixture was transferred into autoclave at 180 °C for 12 h. After cooling to room temperature, the prepared materials were washed by DI water six times and dried at 80 °C over night under vacuum.

To adjust the size and hollow degree of the as-prepared  $\text{MoSe}_2$  nanosphere,

polyvinyl pyrrolidone (PVP) or Pluronic F-127 (block copolymer) were used as the surfactant, respectively. With 20, 50, 100 and 300 mg of F-127, the corresponding products were named as M-1, M-2, M-3 and M-4, respectively.

### **Synthesis of Fe<sub>3</sub>O<sub>4</sub>@PEI nanoparticles**

4 mmol of Fe(acac)<sub>3</sub> and 1 g of polyetherimide (PEI) were dissolved in 30 mL diethylene glycol (DEG) and heated to 120 °C to form a uniform solution. And then, the mixture was heated to 220 °C. After 2 h, the product was cooled to room temperature and washed several times by ethanol and deionized water.

### **Preparation of MFs nanocomposite**

Briefly, the as-prepared sample M-2 were added into Fe<sub>3</sub>O<sub>4</sub>@PEI dispersion with different concentrations (0.1, 0.2 and 0.3 mg mL<sup>-1</sup>). Then the above mixtures were continuously stirring for 12 h at room temperature, the MoSe<sub>2</sub>/Fe<sub>3</sub>O<sub>4</sub> products were gained via centrifugation and marked as MF-1, MF-2 and MF-3, respectively.

### **Detection of ROS**

1 mL of MoSe<sub>2</sub> nanospheres dispersion (300 µg mL<sup>-1</sup>, PBS pH 7.4) with 100 µL ethanol containing 600 µg of dichlorofluorescein diacetate (DCFH-DA) was illuminated with 808-nm NIR laser (1 W cm<sup>-2</sup>). Then, the supernatant was collected by centrifugation and analyzed by fluorescence.

### **Photothermal property**

1 mL of the aqueous dispersion of the as-prepared samples (M-1 ~ M-4, MF-1 ~ MF-3 and pure Fe<sub>3</sub>O<sub>4</sub> nanoparticle, C<sub>samples</sub> = 62.5 ppm) and sample MF-2 with different concentrations were irradiated by 808-nm laser at the power density (1.0 ~

3.0 W cm<sup>-2</sup>), and the temperature was recorded every 1 min by FLIR infrared thermal imager E8.

### **Preparation of MF-2@PEG nanocomposite**

The as-prepared MF-2 (50 mg) and NH<sub>2</sub>-PEG<sub>2K</sub>-NH<sub>2</sub> (1 mg mL<sup>-1</sup>) were mixed within 5 mL of deionized water and stirring for another 24 h at room temperature. Ultimately, the product was collected by centrifugation and named as MF-2@PEG.

### **PFC Loading and oxygen saturation**

After drying, the hollow MF-2@PEG (30 mg) was degassed for 30 min and then filled with 200 μL of perfluorocarbon (PFC) under sonication in the ice-water for 5 min. Subsequently, the above mixtures were placed in a sterile oxygen chamber for 30 min to insure oxygen saturation. And the PFC-loaded and oxygen-saturated MF-2@PEG composite is abbreviated as O<sub>2</sub>@PFC@MF-2@PEG.

### **Measurement of O<sub>2</sub> release**

The oxygen concentrations in aqueous solutions were measured using a portable dissolved oxygen meter (JPBJ-608). To measure the O<sub>2</sub> release, flask contained 10 mL deoxygenated water was filled with nitrogen. Then the oxygen electrode probe was immersed into the water to detect its O<sub>2</sub> concentration in real time. Then, 5 mL of O<sub>2</sub>@PFC@MF-2 or O<sub>2</sub>@MF-2 solution (2.5 mg/mL) was injected into the flask, and then sealed with liquid paraffin. The oxygen concentration was recorded during all processes for 16 min (one measurement every 30 s). For the measurement of O<sub>2</sub> release triggered by NIR laser, the solution was irradiated by a 808-nm laser (1 W cm<sup>-2</sup>) for 5 min.

## Drug loading and FITC conjugation

Firstly, MF-2@PEG (30 mg) and Doxorubicin (Dox, 5 mg) were added to 10 mL of PBS (pH = 7.4) and stirred at room temperature for 12 h. Subsequently, 0.2 mmol of fluorescein isothiocyanate (FITC) was added into above solution, and the mixture was stirred for another 12 h. Ultimately, the precipitate was obtained by centrifugation.

The loading efficiency (LE, wt.%) of Dox can be determined by UV/Vis spectroscopy at 480 nm and calculated by using Equation (S1). The experiment was repeated three times.

$$LE \text{ wt.}\% = \frac{m_{(\text{original Dox})} - m_{(\text{residual Dox})}}{m_{(\text{sample})} + m_{(\text{original Dox})} - m_{(\text{residual Dox})}} \times 100\% \quad (\text{S1})$$

Where  $m_{(\text{original Dox})}$  and  $m_{(\text{residual Dox})}$  stand for the mass of the original and residual Dox in solution, respectively.

## Drug release

MF-2@PEG/Dox nanocomposites (0.6 mg) were dispersed in the PBS (3 mL, pH = 7.4 and = 5.0) in dark or under 808-nm laser irradiation. At the interval time, the corresponding PBS solution was taken out by centrifuging to determine the release amounts by UV-Vis spectrum.

## Cell culture

HepG2 (hepatoma cell line) cells were cultured in monolayers in Dulbecco's Modified Eagle's Medium (DMEM, hyclone) that includes 10% (v/v) fetal bovine serum (FBS, Tianhang Bioreagent Co., Zhejiang) and penicillin/streptomycin (100 U

mL<sup>-1</sup> and 100 mg mL<sup>-1</sup>, respectively, energy chemical) in a humidified 5% CO<sub>2</sub> atmosphere at 37 °C.

### **In vitro cytotoxicity**

The vitro cytotoxicity was assessed by a MTT assay. Firstly, HepG2 cells were seeded into 96-well plates at a quantity of  $7 \times 10^3$  per well in 100  $\mu$ L of the medium for 24 h. Then, the cells were incubated with different concentrations of MF-2@PEG, MF-2@PEG-Dox, O<sub>2</sub>@PFC@MF-2@PEG+GSH (GSH 10 mM), O<sub>2</sub>@PFC@MF-2@PEG+NIR and O<sub>2</sub>@PFC@MF-2@PEG/Dox+NIR nanocomposites. The media was removed after incubated with corresponding materials for 20 h and followed by exposing of 808-nm laser for 15 min. Then, the cells were further incubated for another 4 h. Afterwards, cells were incubated in a medium containing 0.5 mg mL<sup>-1</sup> MTT for another 4 h. The final medium was then replaced with 150  $\mu$ L of dimethyl sulfoxide (DMSO) per well and the absorbance was monitored using a microplate reader (WD-2102A) at the wavelength of 492 nm. The cytotoxicity was expressed as the percentage of cell viability compared to untreated control cells.

### **Fluorescence imaging**

To check drugs release and cellular uptake, HepG2 cells were cultured in a 6-well with the incubation medium (DMEM) for 24 h. Then the cells were incubated with MoSe<sub>2</sub>@PEG and MoSe<sub>2</sub>@PEG-Dox nanocomposites (1 mL, 50  $\mu$ g mL<sup>-1</sup>) for 24 h. After incubation, the cells were stained with calcein-AM and PI for 30 min. For the group of cellular uptake, DAPI was also need to stain cell nucleus. After staining, all

the cells were washed by PBS for 3 times and imaged by using Leica DFC450 C Microsystems Ltd..

### **Intracellular ROS**

HepG2 cells ( $15 \times 10^4$ ) were cultured in a 6-well plate for 24 h, after treatment with MF-2@PEG and O<sub>2</sub>@PFC@MF-2@PEG ( $50 \mu\text{g mL}^{-1}$ , 1 mL) for 5 h, the cells were washed three times by PBS. Then they were cultured with DCFH-DA ( $10 \mu\text{mol L}^{-1}$ ) at 37 °C for 50 min, and the dishes were washed by PBS for another 3 times. After irradiated by 808-nm laser ( $1 \text{ W cm}^{-2}$ ) for 5 min, the DCF fluorescence was imaged by using Leica DFC450 C Microsystems Ltd.

Besides, the intracellular ROS and hypoxia were explored using the ROS-ID Hypoxia/Oxidative stress detection kit. HepG2 cells were cultured in plates at a quantity of  $15 \times 10^4$  in hypoxic or normoxic medium for 24 h. Then, cells were treated with O<sub>2</sub>@PFC@MF-2@PEG or MF-2@PEG for 5 h and then administrated with the kit reagent mix according to the manufacturer's instructions. After 30 min, the cells were washed and irradiated by 808 nm laser for 5 min. After that, cells were washed with PBS and observed by using Leica DFC450 C Microsystems Ltd..

### ***In vitro* and *In vivo* X-Ray CT imaging**

The *in vitro* and *in vivo* CT imaging was conducted on a Philips 64-slice CT scanner (120 kV). *In vitro*, MF-2@PEG composites with various Mo concentrations (0.00, 0.22, 0.44, 0.88, 1.75, 3.50 and 7.00 mg mL<sup>-1</sup>) were placed in 1.5 mL of tubes and then managed in a line for CT imaging measurements. *In vivo*, the 0.1 mL of MF-2@PEG composite with 7 mg mL<sup>-1</sup> of Mo concentration in normal saline was

injected intratumorally for scanning and only normal saline was injected as control group.

### ***In vitro and in vivo T<sub>2</sub>-weighted MR imaging***

The *in vitro* and *in vivo* MR imaging experiments were carried out in a 3.0 T MRI magnet (American GE Discovery MR750 3.0 T magnetic resonance imaging system). *In vitro*, MF-2@PEG composites with various Fe concentrations (0.000, 0.018, 0.037, 0.075, 0.150, 0.300 and 0.600 mM) were placed in 1.5 mL of tubes. After scanning, the  $r_2$  relaxivity values were acquired by the curve fitting of  $1/T_2$  relaxation time ( $s^{-1}$ ) versus the Fe concentration (mM). *In vivo*, the 0.1 mL of MF-2@PEG composite with 0.6 mM of Fe concentration in normal saline was injected to the tumor of mice. MR scan images were taken and only normal saline was injected as control group.

### ***In vivo toxicity***

The mice were purchased from Second Affiliated Hospital, Harbin Medical University, and all the mouse experiments were performed in compliance with the criteria of The National Regulation of China for Care and Use of Laboratory Animals and also compliance with the relevant laws and institutional guidelines of Harbin Normal University and were approved by the ethics committee of the Harbin Normal University. To obtain the transplanted tumor on the mice, H22 cells were implanted in the left armpit of each female Kunming mouse by subcutaneous injection. When the tumor volume is about 8 mm, the mice were divided into five groups ( $n = 5$  group<sup>-1</sup>) randomly. Among them, three groups of mice were injected with 100  $\mu$ L of

saline, MF-2@PEG/Dox and O<sub>2</sub>@PFC@MF-2@PEG/Dox (200 μg mL<sup>-1</sup>, all injected samples were dispersed in normal saline), respectively, and treated with 808-nm irradiation (2 W cm<sup>-2</sup>, 20 min) at 10 h postinjection. To the residual two groups of mice, one group of mice were only injected with 100 μL of saline as the control group, and another group of mice were injected with 100 μL of MF-2@PEG nanomaterial to judge its toxicity. All the treatments were carried out every 2 days for 14 days. Then, the formula:  $V = (\text{length} \times \text{width}^2)/2$  was used to calculate tumor volumes and relative tumor volumes as  $V/V_0$  ( $V$  is tumor volumes in the treatment group,  $V_0$  is tumor volumes in the control group). The body weights and the tumor size were measured and recorded every two days.

### **Histological examination**

After 14 days of treatment, the organs of the heart, liver, spleen, lung, kidney, and tumor tissues of the mice in five groups were excised for histological analysis. Then the excised tissues were dehydrated using buffered formalin, various concentrations of ethanol, and xylene. Subsequently, the dehydrated tissues were encased by liquid paraffin, which sliced and stained with hematoxylin and eosin (H&E). After staining, the slices were observed by optical microscope.

### ***In vivo* immunohistochemical experiment**

To assess the inhibitory effect of O<sub>2</sub>@PFC@MF-2@PEG on hypoxic environment, mouse anti-HIF-1α polyclonal antibody and goat-antimouse IgG antibody conjugated with diaminobenzidine (DAB) were used as primary and secondary antibody, respectively. After photo-treatment with O<sub>2</sub>@PFC@MF-2@PEG

and MF-2@PEG, the tumors were made into tissue sections. By removing paraffin, the above slices of tumor were boiled for 15 min in citrate buffer (0.01 M, pH 6.0), then the endogenous peroxidase was blocked by 3% H<sub>2</sub>O<sub>2</sub> for 30 min. Subsequently, the above slices were incubated with anti-HIF-1 $\alpha$  polyclonal antibody overnight at 4 °C, followed by conjugation to the secondary antibody of goat-antimouse IgG and DAB staining.

### **Characterization**

Transmission electron microscopy (TEM) images of samples were tested by Hitachi H-8100 at an accelerating voltage of 20 kV. Powder X-ray patterns (XRD) were tested on Rigaku Ultima IV diffractometer with Cu Ka radiation (40 kV, 20 mA). UV-Vis spectra were recorded on SHIMADZU UV2550 spectrophotometer. X-ray photoelectron spectroscopy (XPS, VG ESCALAB 220I-XL) were detected with. The fluorescence spectra were surveyed by HORIBA FL-3. A Fourier transform infrared (FT-IR) spectroscopy spectrometer (JASCOFT/IR-420) was used to collect the spectra of these materials. Zeta potential was carried out on a ZetaPALS Analyzer.

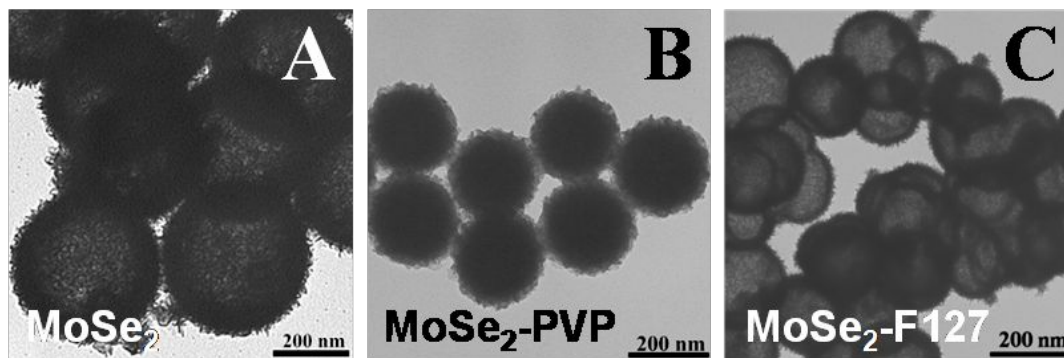


**Figure S1.** TEM images of MoSe<sub>2</sub> nanospheres without surfactant (A), with PVP (B) and with F-127 (C).

MoSe<sub>2</sub> hollow nanospheres (400 nm) assembled by many nanosheets were prepared by a facile one-pot solvothermal method (**Figure S1A**). And then, two kinds of surfactants (PVP and F-127) were introduced to adjust the morphology of products during the sample synthetic procedure. As shown in **Figure S1B-C**, both PVP and F-127 can cut down the particle size from 400 to 180 nm. However, the hollow structure of MoSe<sub>2</sub>-PVP disappeared, which may be due to the hamper of Kirkendall effect with PVP addition. On the contrary, the MoSe<sub>2</sub>-F-127 also remains the hollow structure with the decreased size.

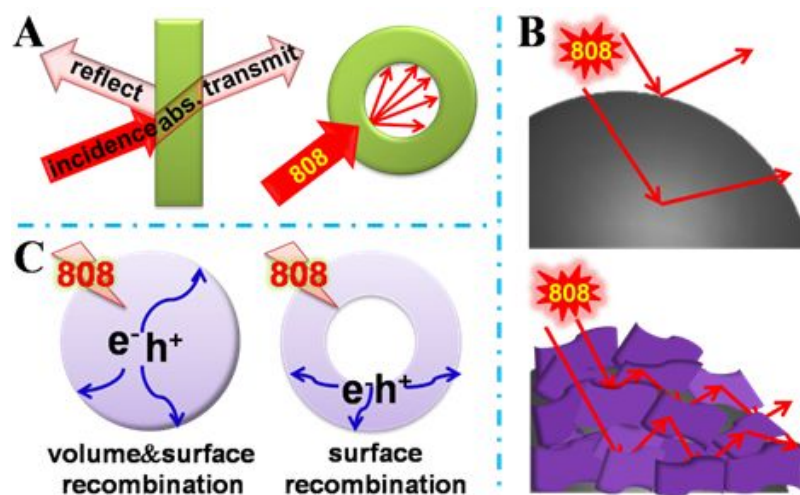


**Figure S2.** (A) Scheme of the light scattering phenomenon on a flat (left) surface and a hollow structure (right). (B) The optical path chart of light on the smooth surface and the rough surface with nanosheets of nanospheres. (C) Charge-transfer model in bulk nanospheres (left) and hollow nanospheres (right).

There are many advantages of the hollow nanostructures with rough surface for PTT and PDT. 1) The novel nanostructure is benefit for the light multi-scattering and multi-reflections facilitating the greater light harvest and utilization in contrast with solid and smooth sample **Figure S2A-B**. 2) Based on the above investigation, the efficient separation of photogenerated electron and hole can promote ROS generation. And the photogenerated electron must migrate to the surface to capture dissolved  $O_2$  making ROS. However, there are many volume and surface recombination in this process. As shown in **Figure S2C**, the hollow structure with thin shell can effectively avoid volume recombination that also benefits to ROS generation.

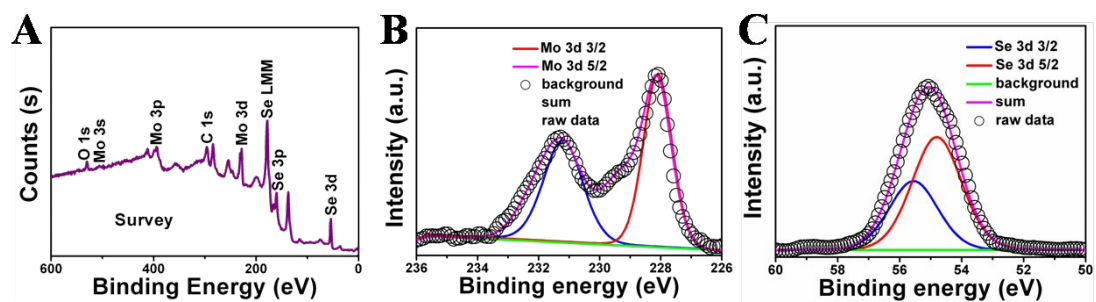


**Figure S3.** XPS survey spectrum (A), Mo 3d spectrum (B) and Se 3d spectrum (C) of the sample M-2.

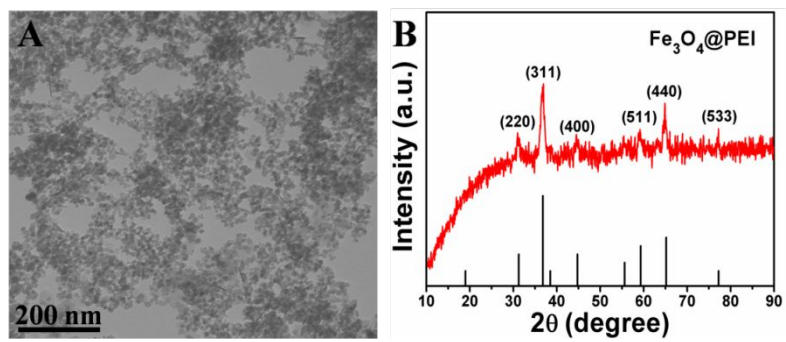


**Figure S4.** TEM image (A) and XRD (B) of as-prepared Fe<sub>3</sub>O<sub>4</sub>@PEI nanoparticles.

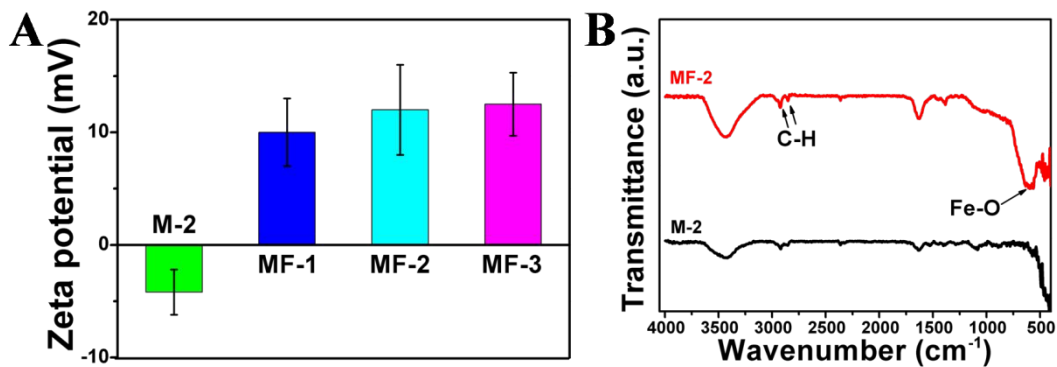


**Figure S5.** (A) Zeta potentials of sample M-2, MF-1, MF-2 and MF-3. (B) FTIR spectra of M-2 and MF-2.

As shown in **Figure S5A**, the electrostatic interaction between MoSe<sub>2</sub> and Fe<sub>3</sub>O<sub>4</sub> nanoparticles was testified by zeta potentials. After the graft of Fe<sub>3</sub>O<sub>4</sub>, the Zeta potential increase due to the positive charge of Fe<sub>3</sub>O<sub>4</sub>-PEI. Besides, the FTIR spectra of M-2 and MF-2 were carried out to further illustrate the construction of MoSe<sub>2</sub>/Fe<sub>3</sub>O<sub>4</sub> heterostructure (**Figure S5B**). Compared with M-2, the emerging characteristic peak (at 606.8 cm<sup>-1</sup>) of MF-2 is ascribed to the Fe-O band, meaning that the Fe<sub>3</sub>O<sub>4</sub> is successfully grafted onto MoSe<sub>2</sub>.

	MoSe <sub>2</sub>	Fe <sub>3</sub> O <sub>4</sub>
MF-1	1	0.032
MF-2	1	0.055
MF-3	1	0.076

**Table S1.** The molar ratio of MoSe<sub>2</sub> and Fe<sub>3</sub>O<sub>4</sub> in the three samples calculated from ICP.

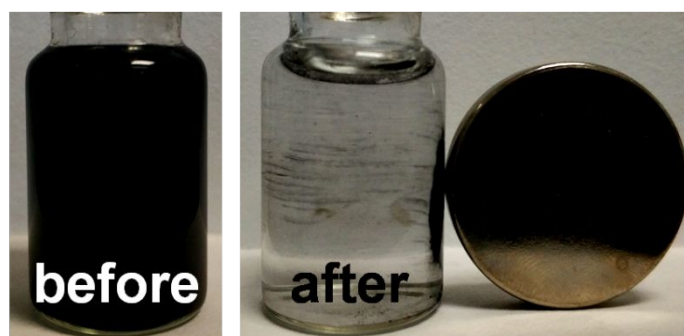


**Figure S6.** Photographs of MF-2 before and after attracted by an external magnet.

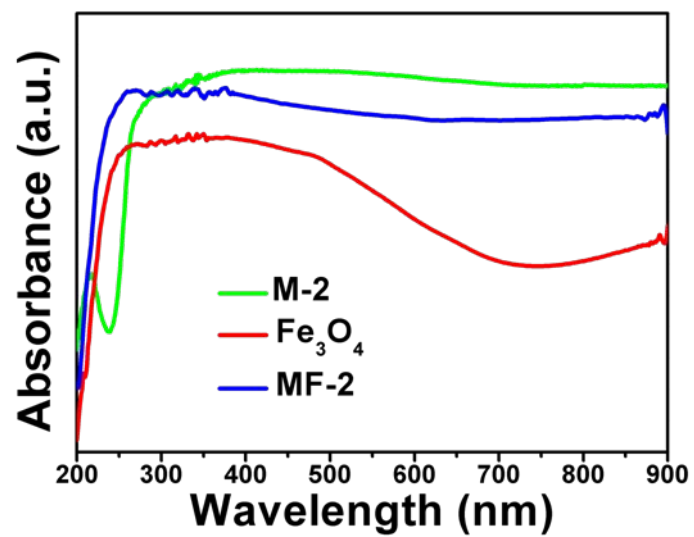


**Figure S7.** The UV-Vis diffuse spectra of the three samples.

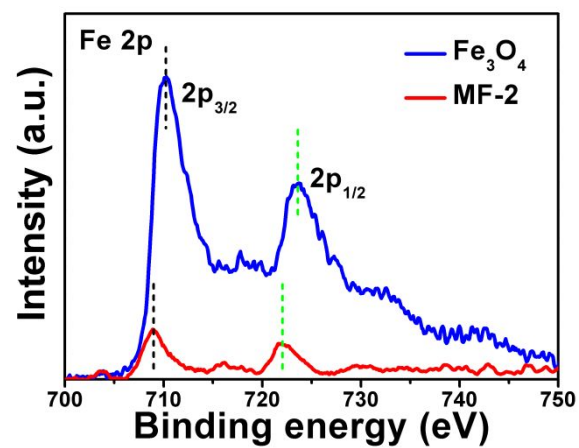


**Figure S8.** XPS spectra of Fe 2p of as-prepared Fe<sub>3</sub>O<sub>4</sub> and MF-2 nanomaterials.

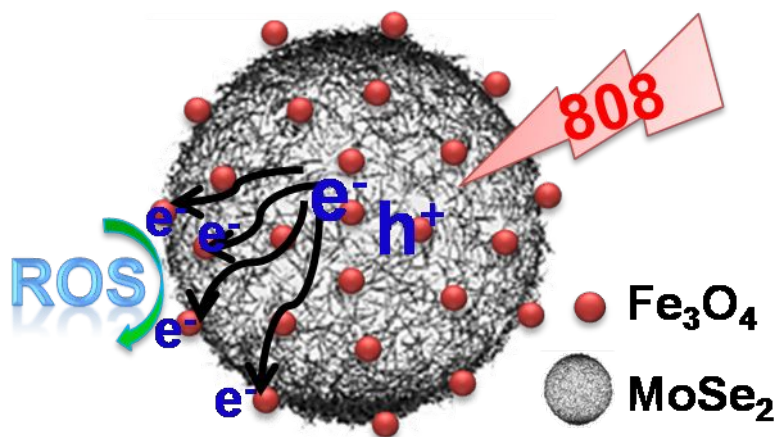


**Figure S9.** Schematic illustration of the charge transport in MoSe<sub>2</sub>/Fe<sub>3</sub>O<sub>4</sub> system.

From **Figure S9**, the Fe<sub>3</sub>O<sub>4</sub> particles on the outer surface of hollow MoSe<sub>2</sub> nanospheres can capture the photogenerated electrons to effectively participate the reaction of ROS production, and it can also weaken the surface recombination of charge.

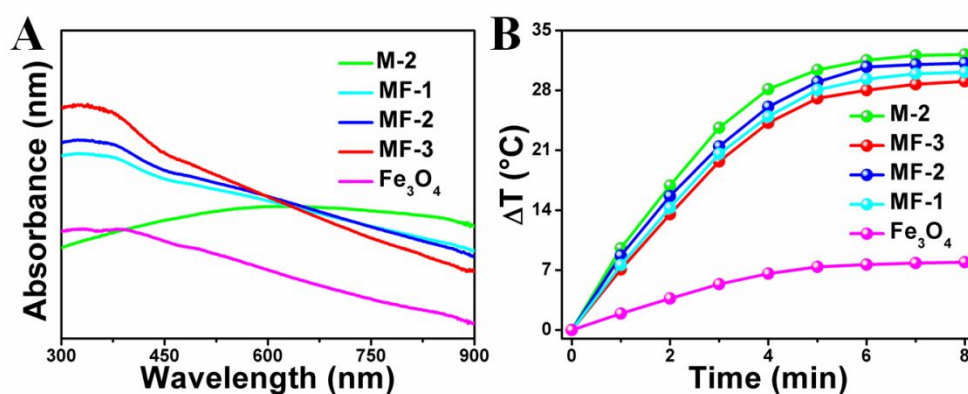


**Figure S10.** (A) UV-Vis spectrum of the five samples. (B) Photothermal heating curves of the five sample dispersions ( $62.5 \mu\text{g mL}^{-1}$ ) under 808-nm laser ( $1 \text{ W cm}^{-2}$ ) irradiation.

As shown in **Figure S10A**, MFs suspensions reveal a decreased absorption compare with M-2, which because of the loading of Fe<sub>3</sub>O<sub>4</sub>. But the photothermal performance of MF-2 is outstanding among the MFs nanocomposites, which also exhibits an ignorable change compared with pure MoSe<sub>2</sub> (**Figure S10B**).

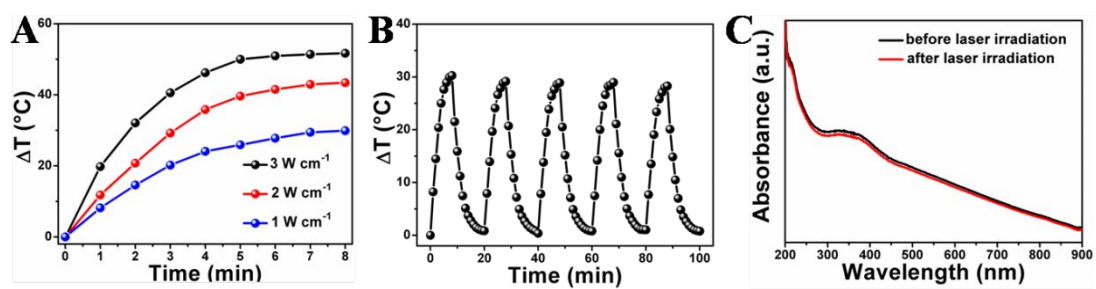


**Figure S11.** (A) Temperature change curves for aqueous dispersions of MF-2 under 808-nm laser irradiation with different power densities of 1, 2 and 3  $\text{W cm}^{-2}$ . (B) Photothermal stability curve of MF-2 nanospheres. (C) The UV-Vis spectrum of MF-2 solution before and after five illumination cycles.

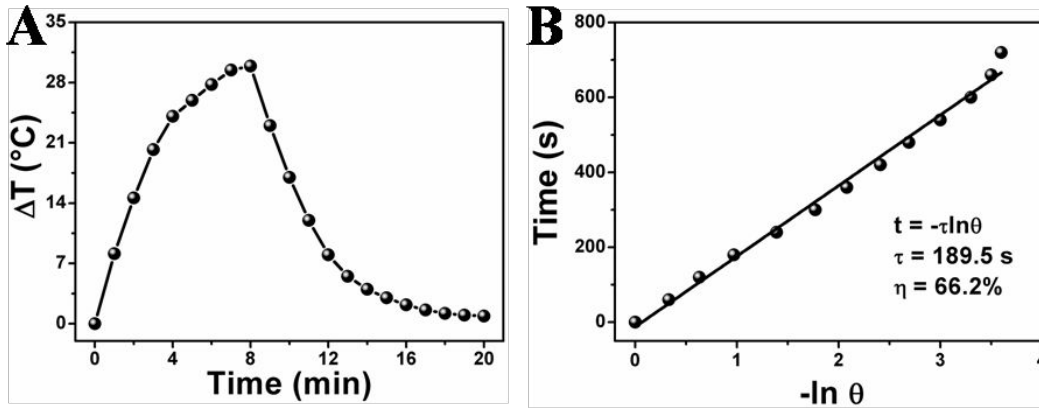


**Figure S12.** (A) Temperature evolution of the dispersion of sample MF-2 during heating (laser on) and cooling (laser off). (B) Thermal equilibrium time constant of MF-2 system determined by fitting the time data versus negative natural logarithm of the driving force temperature from the cooling period.

To test the photothermal conversion efficiency ( $\eta$ ) of MF-2, its aqueous dispersions ( $62.5 \mu\text{g mL}^{-1}$ ) were illuminated under 808-nm laser at the power density of  $1.0 \text{ W cm}^{-2}$ , and temperature changes were recorded as exhibited **Figure S12A**. The photothermal conversion efficiency ( $\eta$ ) is calculated according to formula (S2).

$$\eta = \frac{hA(T_{\max} - T_s) - Q_0}{I(1 - 10^{-A\lambda})} \quad (\text{S2})$$

where  $T_{\max}$  is the maximum temperature of the system,  $T_s$  is the surrounding temperature, and according to **Figure S12A** the  $(T_{\max} - T_s)$  of the sample MF-2 at the power density  $1.0 \text{ W cm}^{-2}$  is  $29.9 \text{ }^\circ\text{C}$ .  $I$  is the power of 808 nm laser (calculation for 1000 mW) and  $A$  is the absorbance of the MF-2 nanospheres suspension at 808 nm.  $Q_0$  is the energy input by the solvent because of the light absorption.  $h$  is the heat transfer coefficient,  $A$  is the surface area of the cuvette, and  $hA$  was confirmed via recorded the drop value of temperature after removing the laser (shown in **Figure S12A**) and according to following formulas.

$$\tau = \frac{m_D C_D}{hA} \quad (\text{S3})$$

$$\theta = \frac{T - T_s}{T_{\max} - T_s} \quad (\text{S4})$$

$$\ln \theta = -\frac{t}{\tau} \quad (\text{S5})$$

Here,  $T$  is the transient temperature of the system during the temperature-fall period.  $\tau$  is the system time constant that can be calculated to be 189.5 s by the linear relationship between cooling time and  $-\ln\theta$  shown in **Figure S12B**.  $m_D$  and  $C_D$  are the mass (1.0 g) and specific heat (4.2 J/g·°C) of the solvent (deionized water), respectively. Then the  $Q_0$  and  $hA$  are calculated according formula (S3).

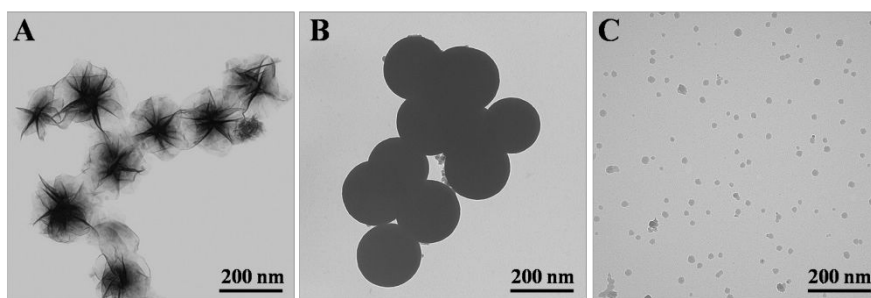


**Figure S13.** TEM images of MoSe<sub>2</sub> nanoflowers (A), solid nanospheres (B) and nanosheets (C).

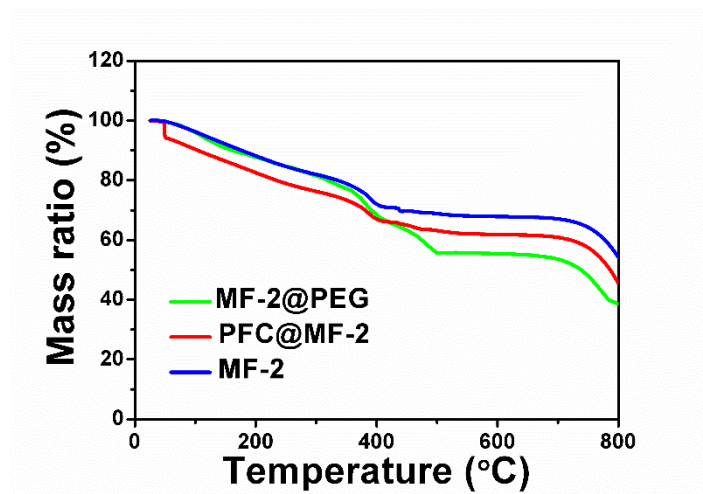
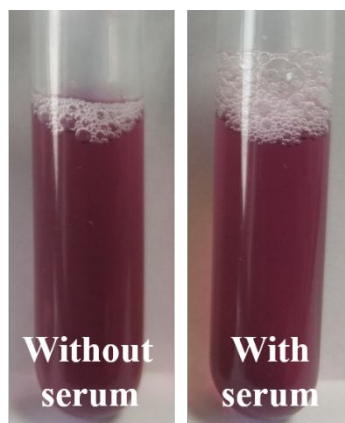
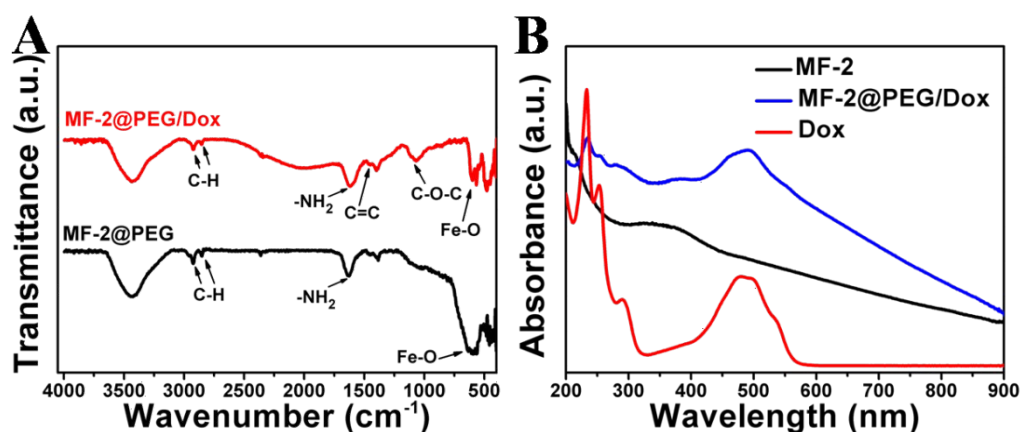


Figure S14. TG curves of the three samples.



**Figure S15.** Photos pictures of  $O_2@PFC@MF-2@PEG$  nanocomposite ( $100 \mu\text{g mL}^{-1}$ ) dispersed in culture medium without (left) and with (right) serum after 3 days' storage.



**Figure S16.** (A) The FTIR spectra of MF-2@PEG and MF-2@PEG/Dox nanocomposites. (B) The UV-Vis spectra of free Dox, MF-2@PEG and MF-2@PEG/Dox nanocomposites.

To improve the biocompatibility and stability of MF-2, NH<sub>2</sub>-PEG-NH<sub>2</sub> (PEG) was conjugated on its surface, and the loading mass ratio of PEG was calculated to be 19% by thermogravimetric analysis (**Figure S14**). Owing to the hollow nanostructure can provide plenty of space, antitumor agent doxorubicin (Dox) was loaded into MF-2@PEG for chemotherapy. As shown in **Figure S16A**, the bands at 2912 (C-H), 1620 (-NH<sub>2</sub>) and 1096 cm<sup>-1</sup> (C-O-C) are due to the PEGylation of MoSe<sub>2</sub>@PEG. The emerging peak at 1458 cm<sup>-1</sup> is ascribed to the C=C band of the aromatic ring structure, revealing the loading of Dox. From **Figure S16B**, MF-2@PEG/Dox reveals a superimposed absorption peak at 485 nm, suggesting the Dox loading.

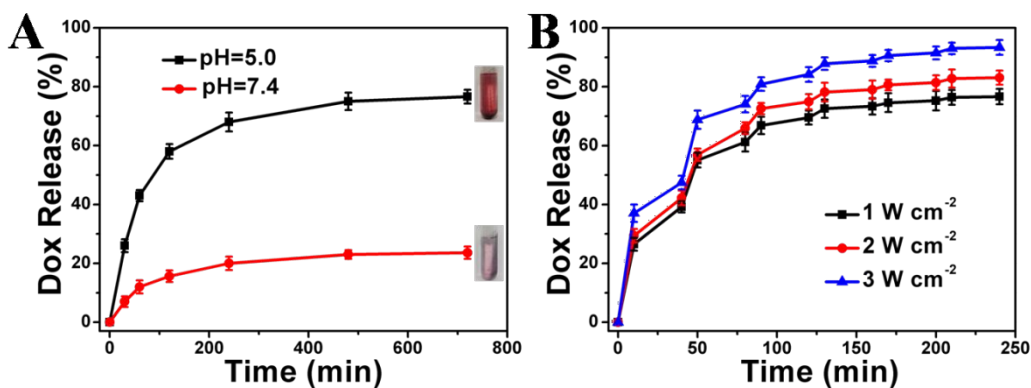


**Figure S17.** (A) The release profiles of Dox from MF-2@PEG/Dox nanocomposites at pH 7.4 and pH 5.0. (B) The release profiles of Dox from MF-2@PEG/Dox at pH 5.0 with alternative 808-nm laser (1, 2 and 3 W cm<sup>-1</sup>) irradiation 10 min/dark for every 40 min.

The Dox release performance was detected via the UV-Vis absorption spectrum at 485 nm. As shown in **Figure S17A**, the Dox release curves of MF-2@PEG-Dox system reveals a weak release ability at pH 7.4 ( $23.6 \pm 2.1\%$ ), however that is improved at acidic condition (pH 5.0) to  $76.6 \pm 2.4\%$  due to the weakened electrostatic interaction under acid condition. The acidic modulated Dox release in MF-2@PEG-Dox is beneficial to the CDT because of the acid condition (pH 4.0 ~ 5.0) in tumour tissue. Furthermore, the photo-triggered Dox release was surveyed as present in **Figure S17B**. When NIR illumination is elevated to 1, 2 3 W cm<sup>-1</sup>, the Dox release can be sharply increased to  $76.8 \pm 2.6\%$ ,  $83.1 \pm 2.2\%$  and  $93.4 \pm 2.6\%$  due to the hyperpyrexia derived from photothermal effect which weaken the  $\pi$ - $\pi$  stacking interaction and accelerate thermodynamic movement of Dox. Therefore, both pH and photothermal sensitive-release performance make MF-2@PEG/Dox as a potential specific chemotherapeutic agent.

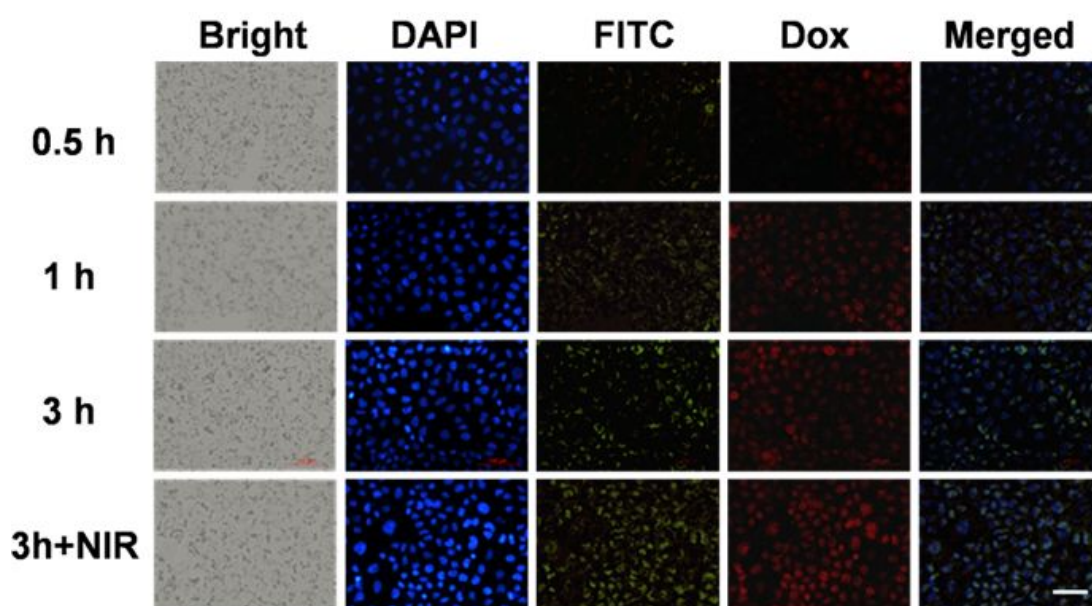


**Figure S18.** Fluorescence images of FITC and intercellular Dox release in HepG2 cells which after incubated with MF-2@PEG/Dox/FITC nanocomposites for 0.5 h, 1 h, 3 h and 3 h+NIR. For each panel, the images from left to right show bright field, cell stained with DAPI (blue), FITC fluorescence (green), Dox fluorescence (red) and the merged. Scale bar: 50  $\mu\text{m}$ .

The intracellular drug release and uptake of MF-2@PEG/Dox/FITC in HepG2 cells is shown in **Figure S18**. The green fluorescence can be found in cytoplasm after the incubation for 30 min, the fast uptake can be ascribed to the nanoparticle size. After illumination by 808-nm laser, the green fluorescence heightens, manifesting that the hyperpyrexia can improve the phagocytosis and pinocytosis of cell. And the intracellular Dox release can be evaluated by the red fluorescence derived from Dox, and the time-dependent red fluorescence lightened in cell is owing to the acid microenvironment in cancer cell. Besides, the illumination-improved Dox release also can be found that is consistent with **Figure S17B**.

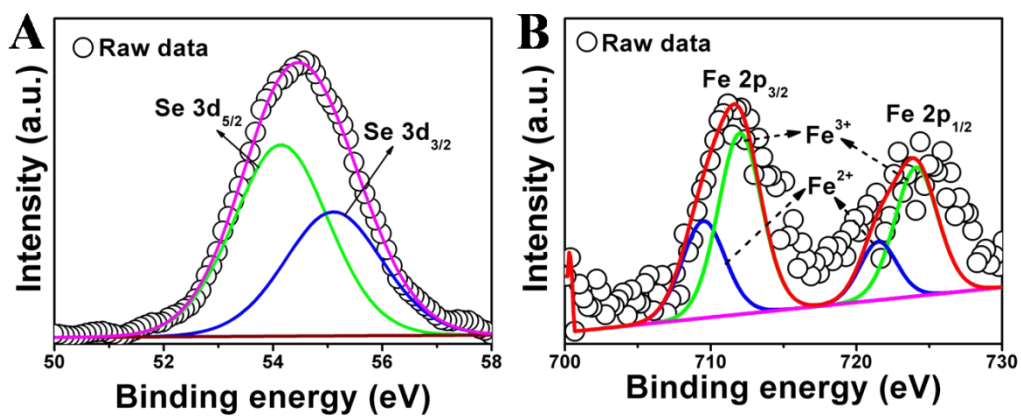
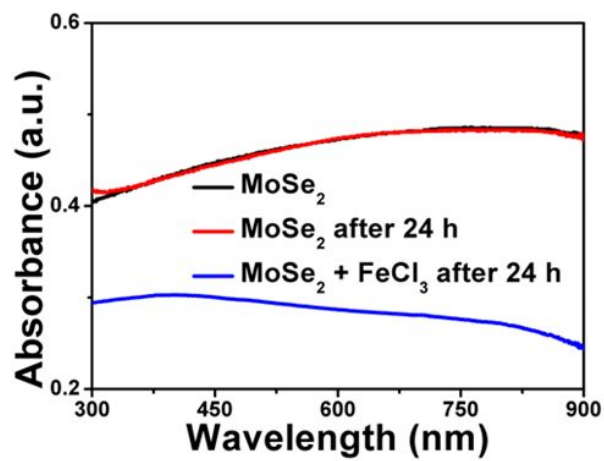
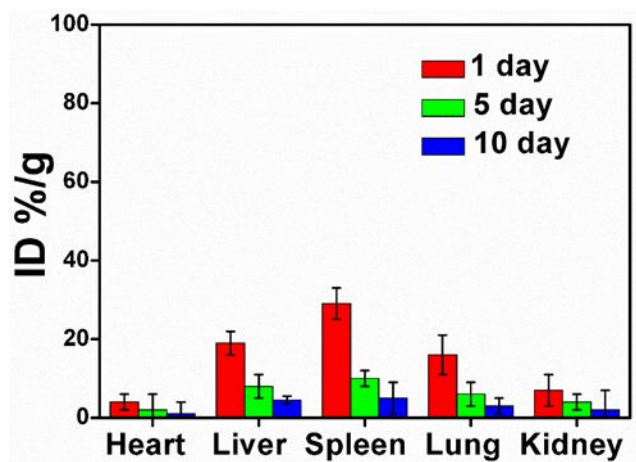


Figure S19. XPS spectra of Se 3d (A) and Fe 2p (B) of MF-2 after degradation.



**Figure S20.** UV-Vis absorption spectra of MF-2 nanocomposites dispersed in CBS and CBS+FeCl<sub>3</sub> solution before and after 24 h.



**Figure S21.** Biodistribution of nanoparticle in major organs after various periods of injection.